

The pressure and temperature dependence of the OH+C₂H₂ reaction above 800 K

Gregory P. Smith, Paul W. Fairchild, and David R. Crosley

Citation: *The Journal of Chemical Physics* **81**, 2667 (1984); doi: 10.1063/1.447976

View online: <http://dx.doi.org/10.1063/1.447976>

View Table of Contents: <http://scitation.aip.org/content/aip/journal/jcp/81/6?ver=pdfcov>

Published by the [AIP Publishing](#)

Articles you may be interested in

The enthalpy change and the detailed rate coefficients of the equilibrium reaction OH+C₂H₂=MHOC₂H₂ over the temperature range 627–713 K

J. Chem. Phys. **97**, 3092 (1992); 10.1063/1.462996

Pressure dependence of the absolute rate constant for the reaction Cl+C₂H₂ from 210–361 K

J. Chem. Phys. **83**, 1005 (1985); 10.1063/1.449463

Erratum: The pressure and temperature dependence of the OH+C₂H₂ reaction above 800 K [*J. Chem. Phys.* **81**, 2667 (1984)]

J. Chem. Phys. **82**, 3473 (1985); 10.1063/1.448987

Pressure dependence of the absolute rate constant for the reaction OH+C₂H₂ from 228 to 413 K

J. Chem. Phys. **73**, 6108 (1980); 10.1063/1.440147

Rates of OH radical reactions. III. The reaction OH+C₂H₄+M at 296°K

J. Chem. Phys. **67**, 674 (1977); 10.1063/1.434871



The pressure and temperature dependence of the OH + C₂H₂ reaction above 800 K

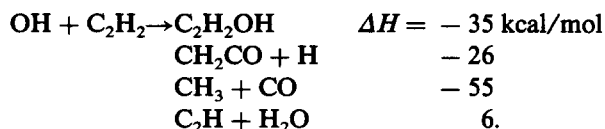
Gregory P. Smith, Paul W. Fairchild,^{a)} and David R. Crosley
Chemical Physics Laboratory, SRI International, Menlo Park, California 94025

(Received 6 March 1984; accepted 16 May 1984)

The rate constant for the reaction OH + C₂H₂ has been measured at 900, 1100, and 1300 K. The experimental method was that of laser pyrolysis/laser fluorescence, in which a pulsed CO₂ laser heats a mixture of SF₆, N₂, H₂O₂, and C₂H₂. The rate constant is determined from the rate of decay of laser-induced fluorescence signals in OH, formed by pyrolysis of the peroxide and consumed by reaction with the acetylene. At the two higher temperatures the rate constant is independent of pressure between 10 and 120 Torr but at 900 K it was observed to be pressure dependent over a similar range. The rate constant at 1100 K is $2.7 \pm 0.6 \times 10^{-3} \text{ cm}^3 \text{ s}^{-1}$, and rises to $5.8 \pm 0.8 \times 10^{-3} \text{ cm}^3 \text{ s}^{-1}$ at 1300 K. Calculations of the temperature and pressure dependence of the addition channel OH + C₂H₂ + M → C₂H₂OH + M were made using Troe's approach, based on flow tube data at a lower temperature. These theoretical calculations are consistent with the present results as well as previous experimental measurements, showing a decrease in the importance of the addition channel with increasing temperature and the onset of a direct route in the region of 1000 K. These considerations of combined pressure and temperature dependence of reaction rates, and changes in mechanism, must be properly taken into account in detailed combustion chemistry models which cover a large range in temperature and pressure.

I. INTRODUCTION

The potential importance of the OH + C₂H₂ reaction in a variety of processes, including the chemistry of soot formation and that of the Jovian atmosphere, has prompted experimental attention over a wide range of temperature and pressure. Studies have been performed both in flow tubes¹⁻⁴ and in flames,^{5,6} yielding widely varying values of apparent Arrhenius parameters and differing conclusions concerning pressure dependence of the rate constant. Various products have been proposed. From the results of these several measurements it is obvious that an unambiguous description of the reaction mechanism and rate constant for the entire temperature range has not been drawn. The data does suggest that, depending on the conditions, more than one mechanism and set of products occur among the many that are thermodynamically possible. These include



There is evidence for the first two channels near room temperature, while the latter three have been deduced in various flame studies.

We have applied a laser pyrolysis/laser fluorescence (LP/LF) method⁷ to investigate the pressure dependence of the rate constant for this reaction at three temperatures intermediate to those of the flow tube and flame experiments. LP/LF presents a reasonably well characterized environment of known composition at elevated temperatures (800–1400 K) for the purpose of making kinetics measurements. LP/LF avoids some of the complications present in deducing rate constants from flame data, and problems due to

walls and reactant pyrolysis which can occur in heated flow tubes. On the other hand, the temperatures are not known as accurately (± 50 K), and heat conduction limits the useful range in time over which measurements can be made. From estimates of expected uncertainties, and a comparison to other studies for the well-known OH + CH₄ reaction,^{7,8} individual rate constants measured by LP/LF should be accurate to 20%–30%. This has proven adequate to establish an understanding of the OH + C₂H₂ reaction.

The first set of measurements, at 1100 K, showed no pressure dependence of the rate constant and a lower value than room temperature measurements at comparable pressures.¹⁻³ This was followed by a theoretical calculation of the addition channel rate constant as a function of *T* and *P*, based on Troe's formalism,^{9,10} to address the consistency of the LP/LF results with those at room temperature, and to select other temperatures for investigation. The subsequent measurements at 900 K, which exhibit a pressure dependence, and those at 1100 and 1300 K which do not, are in full accord with the theoretical calculation.

The picture which emerges includes an addition channel OH + C₂H₂ + M → C₂H₂OH + M, whose rate constant at a given finite pressure reaches a maximum and then decreases with increasing temperature. At temperatures of ~1000 K, a direct channel, probably the abstraction reaction OH + C₂H₂ → H₂O + C₂H, begins to become competitively rapid for pressures of 0.1 to 1 atm. This is consistent with the room temperature measurements, the flame data, and the present experimental results using LP/LF.

This study demonstrates the need to consider the combined pressure and temperature dependence of the rate constant for cases such as this where addition channels are known to occur. These factors must be taken into account to properly incorporate rate constant expressions into models of combustion processes which include detailed kinetics.

^{a)} Present address: TRW Space and Technology Group, Redondo Beach, California 90278.

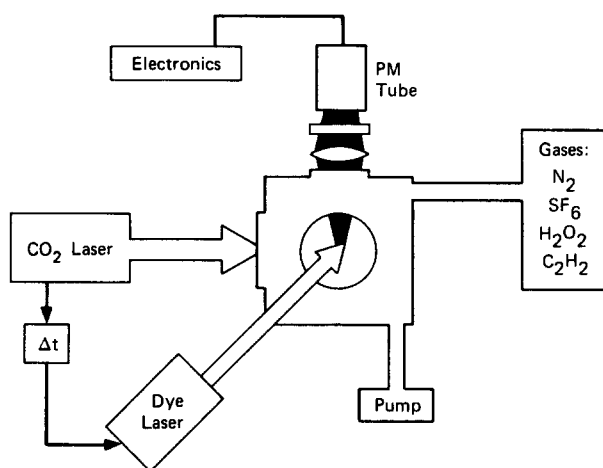


FIG. 1. Schematic diagram of the experimental apparatus. The filter in front of the photomultiplier is a small spectrometer. The time delay Δt is actually controlled by a circuit which fires the lasers sequentially.

II. EXPERIMENTAL MEASUREMENTS

A. Laser pyrolysis/laser fluorescence

The LP/LF method utilizes a pulsed CO₂ laser as the heating source and a pulsed tunable dye laser, fired at a variable time delay after the CO₂ laser, to detect OH radicals via laser-induced fluorescence. The experimental setup is shown in Fig. 1. Details of the LP/LF process and the experimental procedure have been discussed elsewhere^{7,8,11} and a summary will be given here.

A gas mixture, which contains an infrared absorber (SF₆), a bath gas (Ar or N₂), a radical precursor (H₂O₂, with some H₂O present), and the reactant (C₂H₂) flows through a cell and is irradiated with the unfocused 10.6 μm output of a CO₂ laser (1 J/cm² in 1 μs). The SF₆ absorbs the infrared radiation and collisionally transfers this energy to the surrounding gas, rapidly heating the mixture to 800–1500 K. The temperature T attained is set by choice of the CO₂ laser fluence and the SF₆ pressure. Once the gas mixture has been heated, hydroxyl radicals are produced by the thermal decomposition of the peroxide. The dye laser, tuned typically to the P₁₆ line of the A–X (0,0) band of the OH, excites fluorescence which is then filtered with a 0.35 m monochromator and detected by a photomultiplier tube. The signal is processed with a boxcar integrator and plotted on a strip chart recorder. The 2 mm diam probe laser beam and the three-axis geometry used provide point-type probing of the ~ 2 cm diam heated volume, permitting selection of a particular spatial region for performing the kinetic measurements.

By varying the time delay between the lasers, the relative OH density can be mapped as a function of time following the initial heating pulse. By tuning the dye laser through a series of rotational absorption lines, the relative population distribution among ground state rotational levels, and hence the temperature T , can be determined at each time delay. The vibrational temperature of the OH was found to be the same as this rotational temperature,⁸ for delay times used in the kinetics measurements, showing that the system was thermalized. Following the initial heating pulse, an expan-

sion wave traverses the heated region, decreasing both the temperature and density from their initial post-irradiation values. Experimental and computational studies have been carried out to characterize these phenomena.^{7,8,11} After about 20–30 μs , fluctuations in the temperature and density have ceased at the location where the kinetic measurements are made, and remain steady for the 100 μs measurement time. This expansion cooling is typically ~ 200 K, the pressure is now near its original preirradiation value, and further H₂O₂ decomposition stops.

B. Rate constant determinations

The rate of the reaction OH + C₂H₂ for each known added pressure of acetylene, total pressure and temperature was measured from the ratio $\ln(I/I_0)$ as a function of time (30–150 μs). I is the signal from the OH density with added reactant and I_0 the signal from a run under the same conditions with no reactant. The measurements were begun at a long enough time delay following the CO₂ laser pulse to ensure no complications due to the gas dynamics processes. The partial pressure of C₂H₂, set by calibrated flow meters, was typically 0.5–3.0 Torr, large enough relative to OH to assure pseudo-first-order kinetics and to effect a measurable drop in the OH fluorescence signal during the time span of the measurements.

A set of typical runs at one temperature and total added pressure is shown in Fig. 2. The pseudo-first-order rate constants for a series of acetylene pressures is given in Fig. 3. Plots such as these indicated no complicating reactions such as OH + OH, and confirm first order behavior in C₂H₂.

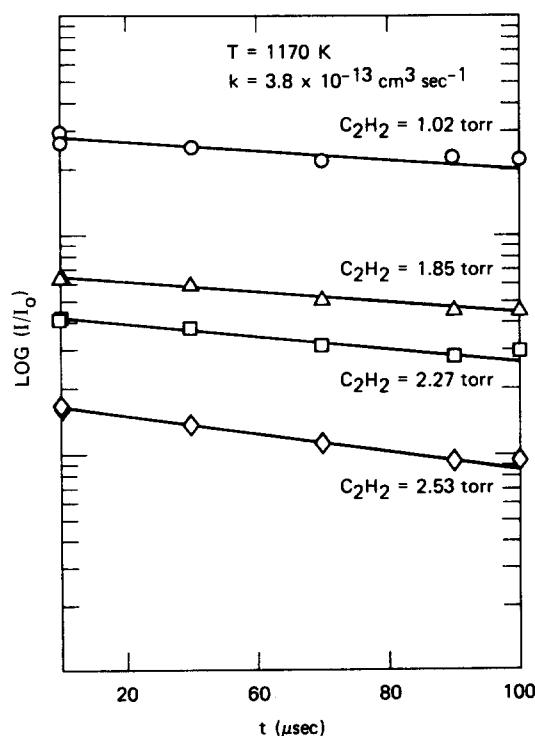


FIG. 2. Logarithmic plots of OH decays in the presence of C₂H₂, referenced to the time dependence of the unreacted OH density, at the conditions indicated. The zero of time on this plot is actually 30 μs after the CO₂ laser fires.

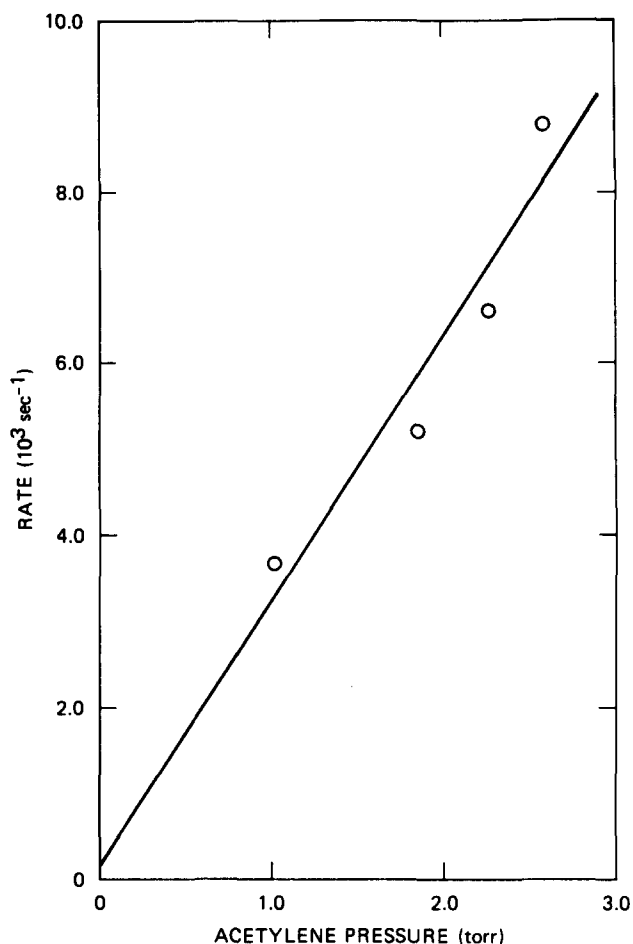


FIG. 3. Sample plot of decay rates vs C₂H₂ pressure, for conditions of Fig. 2.

First order processes such as OH diffusion are compensated for by the $\ln(I/I_0)$ mode of analysis. The actual rate constants were not determined by slopes as in Fig. 3 due to limited experimental C₂H₂ pressure range, but rather by dividing the observed pseudo-first-order rate constants by the acetylene concentration. The values plotted in Figs. 4 and 5 are averages and statistical error bars for each T and P . Typical

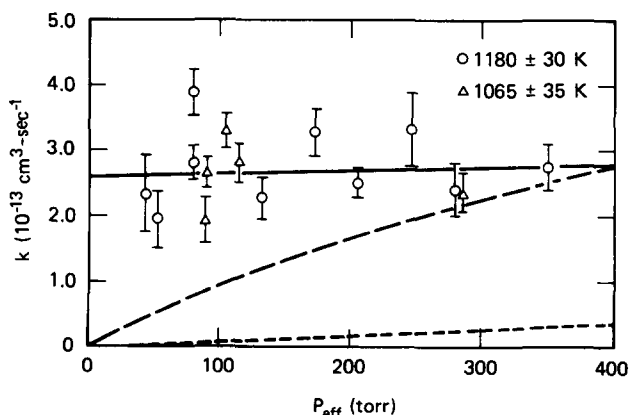


FIG. 4. Measured values of the rate constant at 1180 (circles) and 1065 K (triangles) vs effective pressure. Solid line, least squares fit. Long dashes, calculated prediction for addition channel ignoring adduct equilibrium; short dashes, prediction including equilibrium.

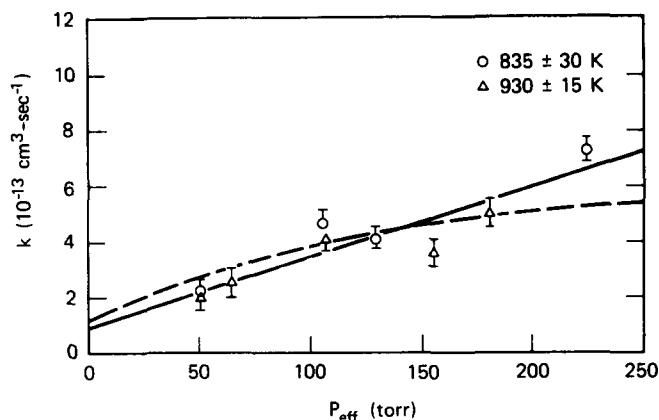


FIG. 5. Measured values of the rate constant at 835 (circles) and 930 K (triangles) vs effective pressure. Solid line, least squares fit. Dashed line, calculated prediction for addition channel plus a direct reaction rate constant of $1 \times 10^{-13} \text{ cm}^3 \text{ s}^{-1}$.

ly three or four measurements were made at different acetylene pressures for each set of conditions.

C. Error estimates

In each run, T is determined by the OH rotational excitation scans. The density of both C₂H₂ and the bath gas are related to the measured pressures in the unirradiated room temperature flows, by means of a computer calculation using a stress wave code available at SRI.¹² Typical errors in the temperature measurement are ± 50 K, the flows are determined to within 5%, and the computation and fluctuation of the temperature-density relationship introduces less than 10% error. These sources of error, together with those arising from noise in the signal and from CO₂ laser intensity fluctuations, lead to an estimate of $\pm 30\%$ error in a given absolute value of a rate constant. A series of rate constant determinations made at the same temperature should have somewhat more precise relative values.

These error considerations are discussed in detail in Refs. 7, 8, and 11. The realistic nature of these estimates is borne out by two observations. First, repeated measurements under the same set of conditions yields results which agree to $\pm 20\%$ or better. Second, rate constants for the previously well-characterized OH + CH₄ reaction have been measured over the range 800–1400 K.⁸ A comparison was made with the expected values, obtained from a fit to more accurate flow tube measurements performed over the range 500–1050 K. The LP/LF results showed rms scatter from the fit of 35%, but an average (signed) deviation of 3%.

III. EXPERIMENTAL RESULTS

A series of rate constant determinations were made over a range of total gas pressure of 10–200 Torr for three distinct temperature regions: 900, 1100, and 1300 K. The results are listed in Tables I–III. In each set there was a spread in temperature somewhat larger than the uncertainty in its determination for each run (± 50 K). However, no statistically significant ordering by temperature within each set was observed. In retrospect, the theoretical results indi-

TABLE I. Results at 1100 K.

	<i>T</i> (K)	<i>P</i> _{eff} (Torr)	<i>k</i> (10 ⁻¹³ cm ³ s ⁻¹)
1	1011	91.9	2.73 ± 0.33
2	1058	89.5	1.94 ± 0.35
3	1082	104.5	3.28 ± 0.35
4	1082	284.9	2.35 ± 0.33
5	1096	113.8	2.84 ± 0.60
6	1149	206.3	2.52 ± 0.43
7	1151	278.8	2.41 ± 0.80
8	1154	64.9	2.49 ± 0.35
9	1168	80.4	3.82 ± 0.39
10	1169	131.5	2.27 ± 0.35
11	1179	43.3	1.77 ± 0.43
12	1188	53.3	1.95 ± 0.38
13	1216	246.6	3.81 ± 0.75
14	1223	349.2	2.75 ± 0.70
15	1237	173.7	3.26 ± 0.40

cate a variation in the rate constant over each set consistent with the experimental error bars, so such a grouping is realistic.

The rate constants are given together with the *effective* pressure of collider gas. This is the equivalent N₂ pressure needed to match the collisional energy transfer rate of a given gas mixture. To attain the same temperature at different total pressures, it was necessary to vary the mole fraction of SF₆ (whose density determined the amount of absorbed CO₂ laser energy and part of the heat capacity) and bath gas of Ar or N₂ (which contributed only to the heat capacity). The effective pressure *P*_{eff} is then given by

$$P_{\text{eff}} = P_{\text{Ar}} + P_{\text{N}_2} + 3P_{\text{SF}_6},$$

which accounts for the approximately threefold greater efficiency of SF₆ in stabilizing an energetic adduct, compared to the similar Ar and N₂ (see below).

The rate constant results from the first set of runs, near 1100 K, is plotted vs effective pressure in Fig. 4. The statistical error bars shown are those obtained from averaging the determinations for each set of conditions; the scatter is in accord with our estimates of anticipated error. No variation can be seen between sets grouped into two temperature ranges.

These results indicate that there is no pressure dependence of the reaction rate constant at 1100 K. An unweighted least-squares fit to the results is shown by the solid line, yielding an intercept (*1σ*) of $(2.6 \pm 0.3) \times 10^{-13}$ cm³ s⁻¹ and a slope of $(0.5 \pm 1.5) \times 10^{-16}$ cm³ s⁻¹ Torr⁻¹, clearly con-

TABLE II. Results at 900 K.

	<i>T</i> (K)	<i>P</i> _{eff} (Torr)	<i>k</i> (10 ⁻¹³ cm ³ s ⁻¹)
1	847	50.0	1.97 ± 0.51
2	928	50.0	2.18 ± 0.51
3	830	69.0	2.59 ± 0.43
4	934	106.8	4.72 ± 0.11
5	869	108.4	4.16 ± 0.25
6	935	128.7	4.17 ± 0.13
7	841	155.1	3.61 ± 0.31
8	788	177.6	5.04 ± 0.10
9	910	223.6	7.34 ± 0.15

TABLE III. Results at 1300 K.

	<i>T</i> (K)	<i>P</i> _{eff} (Torr)	<i>k</i> (10 ⁻¹³ cm ³ s ⁻¹)
	1270	150	5.0 ± 0.4
	1290	160	5.6 ± 0.2
	1360	150	5.8 ± 0.4
	1400	100	7.3 ± 0.5
	1340	105	6.3 ± 0.5

sistent with a lack of pressure dependence. (The dashed lines pertain to the theoretical calculations and will be discussed later). A simple average of all of the results collected at 1140 ± 90 K yields a value for the rate constant for $(2.7 \pm 0.6) \times 10^{-13}$ cm³ s⁻¹. The pressure independence indicates we are here observing a direct channel, perhaps H abstraction, in contrast to the pressure dependent addition channel clearly observed in this pressure range for *T* ≲ 400 K.

Following the indication of the theoretical calculation (presented later) that the two channels may be competitive near 900 K, experiments were performed in that region. The results, again grouped into two sets, are plotted in Fig. 5. Here, a distinct pressure dependence can be seen. Although the rate constant is not expected to be linear in pressure, a least-squares fit was again made to demonstrate that both a nonzero intercept and slope are indicated by the data. The results, shown by the solid line, yield a value of $(0.9 \pm 0.6) \times 10^{-13}$ cm³ s⁻¹ for the intercept and $(2.6 \pm 0.4) \times 10^{-15}$ cm³ s⁻¹ Torr⁻¹ as the slope. (Again the dashed line relates to the theoretical computation.) The addition channel is clearly present and there is evidence for some residual direct reaction at this lower temperature.

Finally, a short series of runs was made near 1300 K. These, given in Table III but not plotted, show no pressure dependence, as expected; they are larger than the value at 1100 K. The result is $(5.8 \pm 0.8) \times 10^{-13}$ cm³ s⁻¹ at 1330 ± 60 K, where again the error (precision) is from simple averaging from each set of runs. This value clearly illustrates that the rate constant is now rising with temperature, indicating a direct process with positive activation energy. The CO₂ laser was operating very near the limit of fluorine atom production from thermal SF₆ dissociation during these high temperature runs. The OH concentrations in the absence of added reactant were less stable and the profiles less reproducible than for the experiments at lower temperature. Hence, the accuracy of these measurements is lower, though difficult to estimate.

IV. THEORETICAL CONSIDERATIONS

Rate constant measurements on the OH + C₂H₂ reaction, including this study, span a temperature range of 230–2000 K and a pressure range from 1–1100 Torr. The results suggest that more than one mechanism and set of products can occur. This raises several questions which can be addressed from the basis of unimolecular and bimolecular transition state reaction theory. Such an analysis can answer some of these questions, draw the varied results toward a unified framework for a better basic understanding as well as

extrapolation to other conditions, and suggest further experiments that need to be undertaken.

A. Mechanistic questions

Of the previous room temperature investigations¹⁻⁴ of this reaction, the recent work of Michael *et al.*³ and Perry and Williamson⁴ covers the widest temperature and pressure ranges (10–1100 Torr, 230–420 K). In the latter work little temperature dependence was found at the highest pressures, while Ref. 3 indicates a more limited pressure dependence and a pressure independent component was inferred for the room temperature reaction. A value¹ at low pressure (1 Torr) and 298 K is also available for comparison. The observed pressure dependence is indicative of a reaction that proceeds by formation of an energized adduct (C₂H₂OH*) that must be stabilized by collisions with a third body to prevent dissociation back to reactants. An attempt to fit these results using unimolecular reaction rate theory can determine whether it is necessary to invoke an additional, direct, pressure-independent reaction channel as well. More importantly, trying to find a reasonable and consistent fit to the data of Refs. 3 or 4 will suggest which set forms the best basis for extrapolating measurements of the addition rate constant to other temperatures and pressures. Extrapolation to higher temperatures should indicate whether one can reasonably expect a contribution from this channel in the current laser pyrolysis experiment, or in flames. If the addition channel is important at the higher temperatures, a second related question concerns the fate of the adduct once collisionally stabilized. Tully¹³ has observed fast, thermal dissociation of the similar [OH + C₂H₄] adduct at 600 K. For acetylene, however, ketene has been observed as a reaction product in a molecular beam experiment,¹⁴ and this rearrangement channel must be examined as an alternate decomposition route. It need not be fast at 298 K to compete with thermal redissociation at higher temperatures.

There are several higher temperature studies, of which this is the only one to directly monitor the disappearance of a reactant. The current work suggests a transition from the addition channel to a direct mechanism near 1000 K. The flame modeling work of Fenimore and Jones,⁵ Brown *et al.*,⁶ and Vandooren and Van Tiggelen¹⁵ supports such a conclusion, although the last group concludes the high temperature products are CH₃ + CO instead of the more likely hydrogen abstraction producing H₂O and C₂H. This question can also be addressed by thermochemical kinetics arguments. Given the potential role of C₂H in soot formation, product identification is a key question that relates to the predicted extrapolation of the direct channel to other temperatures.

B. Theoretical framework

The addition channel for the OH + C₂H₂ reaction forms an energized adduct C₂H₂OH* which is then stabilized by collision with some bath gas molecule M. As the temperature increases, the adduct is formed with a larger excess of energy, and more collisions with M are required in order to stabilize it before redissociation to the original reactants. Hence the falloff region, that is the pressure below

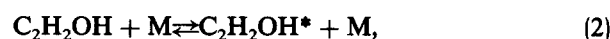
which the overall rate constant is noticeably dependent on [M], moves to higher pressures at higher temperatures. Quantitative consideration of these effects is best carried out by consideration of the reverse reaction, i.e., the unimolecular decomposition of the stable adduct.

The rate constant for the addition reaction k_1 is related to the adduct decomposition rate constant k_{-1} by the equilibrium constant



$$k_1 = K_1 k_{-1}.$$

The pressure dependent unimolecular decomposition can be simply described by the Lindemann–Hinshelwood mechanism



$$k_{-1} = \frac{k_2[\text{M}]k_3}{k_{-2}[\text{M}] + k_3} = \frac{k_3K_2}{(1 + k_3/k_{-2}[\text{M}])},$$

with $k_\infty = k_3K_2$ rate determining at high pressure and $k_0 = k_2$ at low pressure. Since these rate constants are energy dependent and the adduct is formed with a distribution of energies, a more complex RRKM treatment integrating over energy is required. The falloff behavior can be successfully approximated by the treatment of Troe,^{9,10} whose Eq. (4) has been used to predict the pressure falloff behavior analogously to RRKM results:

$$\log k_{-1} = \log [k_0 \text{M} / (1 + k_0 \text{M} / k_\infty)] + \log F_T / [1 + (\log k_0 \text{M} / k_\infty)^2]. \quad (4)$$

F_T is a correction to the Lindemann–Hinshelwood falloff based on a Kassel integral approach and is calculable from adduct thermochemical properties (which are also needed to calculate k_0). Here $k_\infty = k_3K_2$ and $k_0 = k_2$. The second term in Eq. (4) is dominant for the conditions of Refs. 3 and 4.

Values of k_∞ are easily calculated from the properties of the transition state using activated complex theory:

$$k_\infty = \frac{kT}{h} \frac{Q^\ddagger}{Q} e^{E_0/kT} = \frac{kT}{h} e^{\Delta S^\ddagger/R} e^{-E_0/kT}, \quad (5)$$

where E_0 is the barrier to dissociation and Q^\ddagger is the transition state partition function.

The low pressure limit rate constant is given by

$$k_2 = \beta k_{LJ} F_c \int N(E) e^{-E/kT} dE / Q, \quad (6)$$

where k_{LJ} is the Lennard-Jones collision rate constant of M and the adduct, β is a collision efficiency term for energy transfer, F_c is an angular momentum conservation correction to the nonrotational energy needed for dissociation, and $N(E)$ is the density of states for the adduct at energy E . This integral can be approximated, from the adduct properties, by a procedure developed by Troe.⁹ These same parameters are used in determining the falloff parameter F . Note that since most of the existing low temperature data for this reaction are close to the high pressure limit, it is this calculation of k_0

that is the most theoretical and least accurate portion of the fitting and extrapolation procedure.

C. Parameters used in the calculation

The choice of parameters for this task is somewhat subjective, in terms of both the range of theoretically reasonable values and judgments as to which fit is best and which data points should receive the greatest weight. Variation in one parameter can often be compensated for by another. The process is an iterative one. For clarity, we will present our choices of parameters that generate our best fit to the data of Michael *et al.*,² and present these results. Considerations of alternate parameters, alternate fits, fits to other data, conclusions on the thermal reaction mechanisms, and extrapolation of the addition pathway rate constant to higher temperature will follow.

The structure and stability of the C₂H₂OH adduct are key parameters in calculating k_0 (and F), and in choosing the configuration of the related transition state for k_∞ . Values used are given in Table IV. The vibrational frequencies involving oxygen are taken from methanol, while the CH and CC values are from ethylene.¹⁶ The moments of inertia are derived for a planar complex with 1.07 Å CH bond lengths, a 1.34 Å CC bond length (from ethylene), a 1.36 Å CO bond length, a 0.96 Å OH bond length (from methanol), and 120° HCC–H and HCC–OH bond angles.¹⁷ With an electronic degeneracy of 2, this gives a entropy of 63.8 e.u. at 298 K, close to the 64.5 e.u. value for the CH₃CO isomer.¹⁸ The low frequencies (300 cm⁻¹) involving OH torsion are the key parameters. A possible tightening to 400 cm⁻¹, attributable to partial double bond character in the CO bond, would only drop S_{298} by 0.8 e.u., a factor of 1.5 in K_1 .

The enthalpy of the adduct is more difficult to estimate. One basic thermochemical argument, with a probable error of ~5 kcal/mol, is given by Michael *et al.*³ Assuming the C–OH bond energy in vinyl alcohol is the same as the 109 kcal/mol value¹⁹ for formic acid, ΔH_f° for vinyl alcohol is –30.5 kcal/mol. Using a 110 kcal/mol CH bond energy for both ethylene and vinyl alcohol, ΔH_f° of the adduct is 27.5 kcal/mol and it is stable by 36 kcal/mol with respect to OH + C₂H₂. Tully's observation¹³ of equilibrium at 591 K for the similar OH + C₂H₄ adduct, coupled with an estimate

of 66.2 e.u. for S_{298} ($S_{591} = 80.4$ e.u.), gives $a \sim 31$ kcal/mol stability for that related species. We chose 35.7 (± 5) kcal/mol = ΔH_{298} ; $\Delta H_0 = 34.0$. This may be compared with a value of 30.4 kcal calculated with an empirically corrected *ab initio* method.²⁰

A few other parameters are needed for k_0 and F . Thermodynamic values for OH and C₂H₂ are taken from JANAF.²¹ The Lennard-Jones parameters for ethanol are used for the adduct.²² Collision efficiencies can be calculated⁹ from values of the average energy transferred per collision ΔE , which depends upon the bath gas M. Recent photochemical studies²³ indicate a 0.4 kcal/mol value for Ar, but chemical studies²⁴ show a wide range of values. Thus ΔE is in a sense a fitting parameter, within reasonable bounds of 0.25–1.0 kcal/mol. Our best fit used a 0.36 kcal/mol value for ΔE , which gave a reasonable efficiency β of 0.26 at 298 K. Finally, the centrifugal energy term F_c is fully incorporated into the Troe k_0 formalism,⁹ and uses the I^\ddagger/I from transition state theory. This term is only a minor one in this case.

Existing data for k_∞ restrict the choice of the transition state. The results of Ref. 4 and especially Ref. 3 show a positive temperature dependence, indicating a small energy barrier to recombination, as might be expected for a radical-molecule addition process. The presence of such a barrier argues in turn for a tight transition state, where the C–OH bond is not extended and the OH torsions are closer to the adduct frequencies than they are to the 65 cm⁻¹ value which represents the entropy of a free OH rotor¹⁸ at 298 K. Furthermore, the low values of k_∞ indicate that even with no barrier, ΔS^\ddagger must be low. At 298 K, $k_\infty = 8 \times 10^{-13}$ requires $\Delta S_{-1}^\ddagger < 6$ e.u. (decomposition direction) for barriers under 2.5 kcal/mol. While specifying a tighter adduct could increase ΔS^\ddagger by ~1 e.u., a loose transition state, as in fission to two radicals, would have $\Delta S^\ddagger > 11$ e.u. and also would predict a negative temperature dependence. Our best fit k_∞ , corresponding closely to the Arrhenius parameters of Michael *et al.*² ($E_a = 1.3$ kcal/mol), is derived from the transition state given in Table IV, with a $E_0^\ddagger = 1.2$ kcal/mol barrier to recombination. The average ratio of moments of inertia I^\ddagger/I of 1.32 results from $a \sim 0.37$ Å extension of the C–OH bond in the transition state, near the typical 0.4 Å value.¹⁸

TABLE IV. Calculation parameters for reaction (1).

Mode	Adduct	Transition state
CH stretch (2)	3000 cm ⁻¹	3000 cm ⁻¹
CH bend (2)	1300	1300
CH bend	600	600
CC stretch	1600	1600
OH stretch	3600	3600
OH bend	1300	1300
CO stretch	1000	...
CCO deformation	300	205
OH torsion	300	205
I	54.5 amu Å ²	67.1 amu Å ²
	5.9	8.8
	60.5	76.1
ΔE_0^\ddagger	–34.0 kcal/mol	+1.2 kcal/mol
$I^\ddagger/I = 1.32$		$\Delta E = 0.36$ kcal/mol
$\alpha_{LJ} = (3.42 + 4.46)/2$ Å		$\epsilon_{LJ} = \sqrt{124.391}$ K

D. Fits to low temperature data

The resulting fit to the data of Michael *et al.*² is shown as the solid lines in Figs. 6 and 7. Numerical results are given in Table V. Except for the 257 K results, a good fit is obtained. Small discrepancies exist for the lowest pressure points at 228 and 298 K, and intermediate pressures at 362 K, but the agreement is good at the highest temperature data where the falloff, and thus the sensitivity to these calculations, is greatest. Furthermore, the parameters (Table IV) used for this fit all have extremely reasonable values.

The data of Ref. 3 do not extend below 10 Torr pressure where, according to the calculations, the pressure falloff of k_1 is very steep for the lower temperatures. A single point was measured by Pastrana and Carr,¹ at 1 Torr pressure and

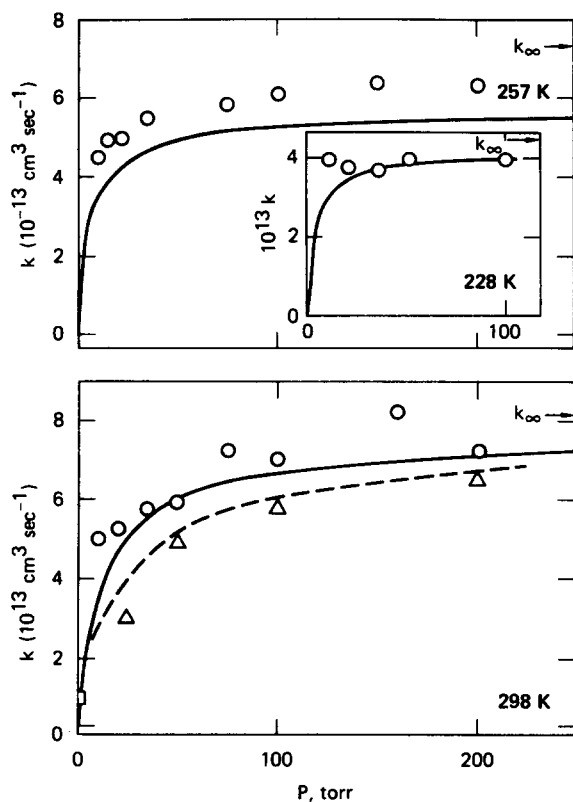


FIG. 6. Rate constant results from Ref. 3 (circles) and Ref. 4 (triangles) as a function of pressure at three low temperatures. The square on the 298 K plot is the 1 Torr point of Ref. 1. Solid line, values calculated values from the theoretical fit, based on the points of Ref. 3. Dashed line, alternative fit based on results of Ref. 4.

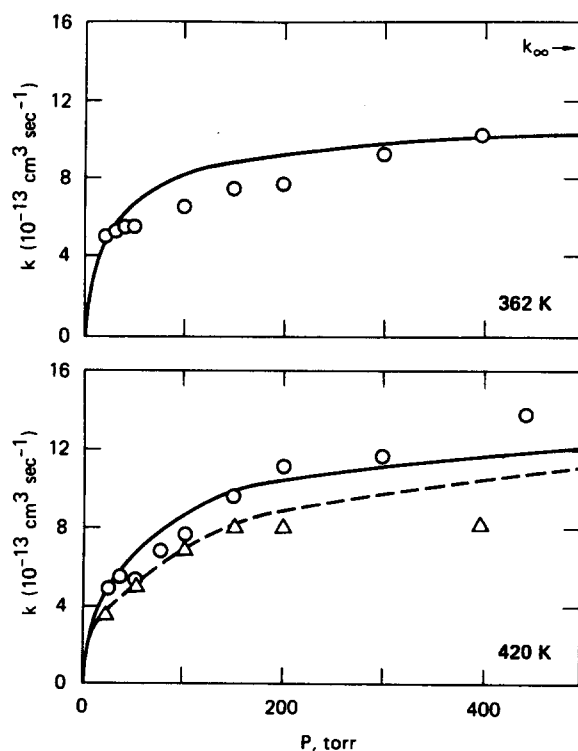


FIG. 7. As in Fig. 6 for two higher temperatures. The "420 K" points of Ref. 3 are actually at 413 K and those of Ref. 4 at 429 K.

TABLE V. Calculation results for reaction (1).

T (K)	K_1 (cm ⁻³)	k_0 (10 ⁻³⁰ cm ⁶ s ⁻¹)	k_∞ (10 ⁻¹¹ cm ³ s ⁻¹)	F_T
228	4.01×10^{-9}	5.616	0.45	0.686
257	2.24×10^{-5}	5.770	0.60	0.657
298	2.58×10^{-1}	5.568	0.83	0.619
362	8.30×10^3	4.747	1.19	0.567
413	3.27×10^6	3.969	1.48	0.530
600	1.8×10^{12}	1.775	2.51	0.425
800	2.5×10^{15}	0.718	3.63	0.355
1000	1.89×10^{17}	0.302	4.87	0.312
1200	3.15×10^{18}	0.134	6.26	0.285
1400	2.25×10^{19}	0.063	7.86	0.269

room temperature (included as the square in Fig. 6), and agrees with the theoretical calculation. Although the value obtained in Ref. 1 is subject to some uncertainty due to the method of analysis, it is significantly lower than the results of Ref. 3 for pressures above 10 Torr. Taken together, these measurements are consistent with the steep falloff indicated by the calculation.

The 257 K data can be fit using a higher k_∞ , although this would be inconsistent with the present transition state theory approach. Attempts to alter the transition state by decreasing the barrier and tightening the vibrations result in a poorer overall fit. While the 257 K match improves, theory would then predict higher values than the measured data at 228 K and lower values than the 420 K results.

The parameters of the transition state, in particular ΔE_0^\ddagger for reaction (1) and S^\ddagger , are largely fixed by the experimental data. In the absence of low pressure data, however, there is considerable uncertainty in k_0 and the adduct parameters which determine its value. [Note that $k_\infty(1)$, but not $k_\infty(-1)$, is independent of adduct parameters.] A similar fit, and similar value of k_0 , can be obtained by raising the adduct dissociation energy and lowering the energy removed per collision, or vice versa. Alternate values for example are $\Delta E_0^\ddagger = 35.0$, $\Delta E = 0.26$ kcal/mol. Similarly, raising the 300 cm⁻¹ adduct frequencies, or lowering I^\ddagger/I , can be compensated for by raising ΔE_0^\ddagger .

Variations on the fit, using different k_∞ and k_0 values, are possible within limits. At 298 K for example, an 8% change in k_∞ and a 28% change in k_0 , in opposite directions, still gives an acceptable fit. Such alterations however produce poorer agreement over the complete temperature range. A second set of pressure dependent data, from Perry and Williamson's study,⁴ is also shown in Figs. 6 and 7. (The data included on the graph labeled 420 K were actually taken at 413 and 429 K.) The previous fit does a passable job for this data also. The best fits, to this data alone, given by the dashed lines, use $\Delta E_0^\ddagger = 34.0$ and $\Delta E = 0.26$ kcal/mol to give $k_0 = 3.0 \times 10^{-30}$ and 2.3×10^{-30} cm⁶ s⁻¹, with the same k_∞ values. We note that the highest pressure point at 429 K cannot be fit well. There are two theoretical reasons to question this value. As the temperature rises, the falloff region should shift to higher pressures. This is because β , $[M]$, and term $N(E)dE/Q$ all fall with T [see Eq. (6)]. The data of Ref. 4 fail to show this trend. Secondly, the small tempera-

ture dependence of k_{∞} reported in Ref. 4 cannot be fit by a reasonable transition state model. It requires a model with virtually no barrier for addition, and a ΔS^{\ddagger} which declines with increasing T . Furthermore, the low value of k_{∞} at 298 K would then require a transition state entropy ~ 2.4 e.u. tighter than the adduct itself. Barrierless transition states, however, are typically loose.¹⁸

The fits to these two data sets, and fits in between, summarize the best current knowledge of the rate constant for reaction (1) and the theoretical basis for extrapolation to other pressure and temperature conditions. Measurements are still needed to lower pressures and at between 600–800 K temperatures. The fit to the data of Ref. 3 was chosen for extrapolation since it is the more extensive data set and better shows the theoretically expected results.

It is apparent from these results that 80%–100% of the OH + C₂H₂ reaction observed at 298 K can be ascribed to the pressure dependent addition channel. It is not *necessary* to postulate a direct, rearrangement pathway producing significant quantities of CH₂CO + H or any other exothermic products. Such channels might of course be important above 450 K. The molecular beam experiment⁶ which did observe ketene as a direct product could not observe a pressure stabilized addition channel, and did not estimate yields. These fits of the pressure dependent data indicate ketene production is likely a minor channel at 298 K at most pressures, but should become the major, although slow, product channel at low enough pressures.

E. Addition channel at higher temperatures

The addition model developed to fit the 228–413 K data can be extrapolated to higher temperatures, to determine whether this channel remains important at combustion temperatures. Several values for K_1 , k_0 , k_{∞} , and F_T are given in Table VI up to 1400 K. This is a guide as to whether the addition mechanism should be considered and not a substitute for actual higher temperature measurements. Factor of 2 errors are quite possible given the long range of temperature extrapolation. In particular, at the higher temperatures and pressures less than 1 atm, reaction (1) is close to the low pressure limit; note that it was the low pressure limiting rate constant k_0 that was the least precisely determined quantity from the fit of the lower temperature data. Figure 8 shows the calculated results for k_1 vs temperature at 100 and 760 Torr Ar. At high temperatures k_0 and thus k_1 drop sharply with temperature as the terms of Eq. (6) decrease.

The dashed line in Fig. 6, plotted together with the LP/LF results, is the theoretically predicted rate constant using

TABLE VI. Adduct decomposition.

T(K)	k_D (s ⁻¹)		Adduct fraction [C ₂ H ₂ OH]/[C ₂ H ₂]	
	760 Torr	100 Torr	760 Torr	100 Torr
800	2.3×10^3	8.5×10^2	3.6	0.47
1000	1.0×10^5	3.2×10^4	0.039	0.005
1200	1.1×10^6	2.5×10^5	0.002	2.6×10^{-4}
1400	4.5×10^6	7.9×10^5	2.3×10^{-4}	3.1×10^{-5}

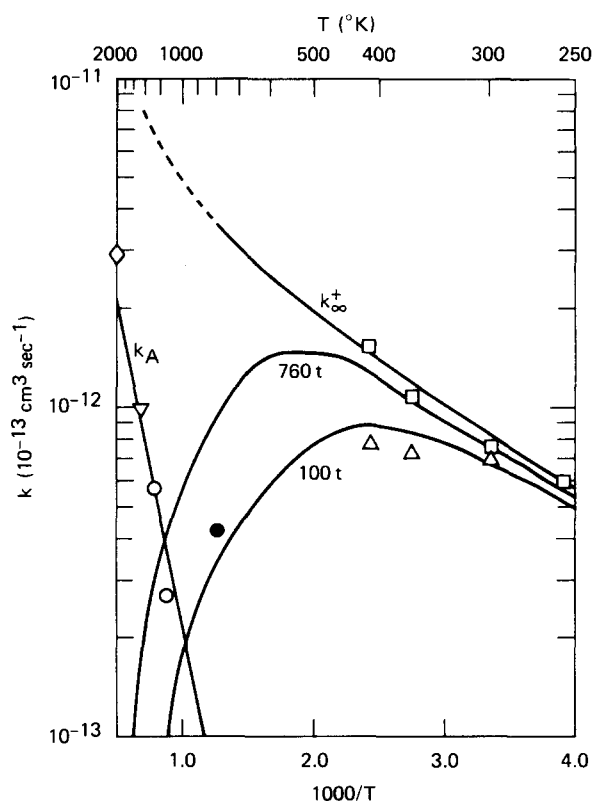


FIG. 8. Overall rate constant results in $\ln k$ vs $1/T$ form. Triangles, 100 Torr points of Ref. 3; squares, points at highest pressure measured in Ref. 3. Diamond, flame measurement of Ref. 5; inverted triangle, flame measurement of Ref. 6. Circles, LP/LF results. Solid circle is the experimental rate constant value at 100 Torr and open circles are the pressure independent values. k_{∞}^+ line is a transition state theory high pressure rate constant which fits the data of Ref. 3. The 760 and 100 Torr lines are the predictions from the computational fit for these pressures. The direct channel line k_A is drawn for an A factor of 2×10^{-11} cm³ s⁻¹ and an E_a of 9 kcal/mol.

this extrapolation plus a 1×10^{-13} cm³ s⁻¹ rate constant for a direct abstraction channel. This shows excellent agreement with the LP/LF data and supports the experimental interpretation and the extrapolation procedure. The solid circle of Fig. 8 also illustrates the agreement of the experimental result at 100 Torr and 900 K with the calculated value.

Given these caveats, and the fact that both the flame gases at 760 Torr and the LP/LF mixture at 100 Torr are roughly twice as efficient collision mixtures as pure Ar, the extrapolation indicates the addition channel may persist to high temperatures. Rate constants near 10^{-13} cm³ s⁻¹ are predicted for the laser pyrolysis experiments in the 800–1200 K range. It is thus reasonable to observe a transition from the pressure dependent addition channel to a different, direct mechanism in our experimental temperature and pressure range. Possible products and rates will be considered later. These results also indicate that under flame gas conditions at 1 atm the [OH + C₂H₂] adduct could be significant up to ~ 1500 K. The fate of such a relatively unstable (~ 35 kcal) adduct at high temperatures will be considered shortly. Further kinetics experiments on this addition reaction near 1000 K and higher total pressure are needed to clarify the decline of the addition channel and establish more accurate rate constants than this extrapolation procedure or the limited pressure range of the LP/LF experiments can provide.

F. Fate of the adduct at high temperatures

At the higher temperatures considered in this study, the addition product, with its low bond dissociation energy, is not thermally stable on microsecond time scales. Two fates are possible: decomposition to the original reactants or stabilization followed by rearrangement of the adduct to an isomeric form which will eventually decompose to different products. The net effect of the first possibility is the establishment of an equilibrium between reactants and adduct, and a substantial reduction of the net addition channel reaction rate in the overall kinetics. The most likely rearrangement channel³ involves a hydrogen migration from oxygen to the β carbon, with subsequent α hydrogen elimination: HOCHCH \rightarrow OCHCH₂ \rightarrow H + OCCH₂. (CH₃ + CO production requires a second hydrogen migration). We emphasize that in this discussion we are considering subsequent thermal reactions of *stabilized* adducts, not direct reactions of initially formed HOCHCH* (as for example, to ketene).

Using the equilibrium constants in Table V and the recombination rate constants at 760 and 100 Torr shown in Fig. 8, the decomposition rate constants given in Table VI can be calculated. Also tabulated are the adduct equilibrium fractions [C₂H₂OH]/[C₂H₂] for 0.1% OH and C₂H₂ concentrations. These values are derived from K_1 and thus are based largely on the value of ΔE_0^\ddagger which in turn was determined with considerable imprecision by the k_0 value used to fit the falloff. A 5 kcal/mol variation in ΔE_0^\ddagger would produce over an order of magnitude change in K_1 and in the values of Table VI.

The calculated results give adduct decomposition rate constants on the microsecond time scale above ~ 1000 K. The low adduct concentrations predicted above this temperature suggest the relative unimportance of this species, and of reaction (1), under the flame and LP/LF conditions modeled by this calculation. This is due to the decomposition reaction, and is valid only if rearrangement is not faster. In the current experiments above 1000 K, a low equilibrium adduct concentration may be established in the 30–40 μ s before the OH disappearance rate measurement is begun. Thus given a direct reaction channel of comparable rate, the declining pressure dependent reaction rate would not be detected. Under flame conditions, the adduct need be considered only if bimolecular reaction is possible on a 100 ns time scale. One suggested possibility⁴ is O₂ + CH₂COH \rightarrow HO₂ + CH₂CO, which is consistent with low temperature flame observations¹⁵ of ketene. The collision rate with 1 Torr O₂ at 800 K is $\sim 10^7$ s⁻¹.

Above 1000 K and at/or below 760 Torr, the adduct decomposition reaction and any rearrangement reaction of comparable rate are very near their low pressure limits. From Eq. (6) one sees that only the difference in the barrier height E_0 for the two channels will determine which predominates. The rearrangement barrier can be estimated only roughly. The ring strain energy involved in the four center transition state for hydrogen migration is approximately 27 kcal/mol from cyclobutane.¹⁸ Adding a typical 7 kcal/mol activation barrier for hydrogen abstraction,¹⁸ we get an activation energy for rearrangement of ~ 34 kcal/mol. This sug-

gests rearrangement might compete with dissociation, but the very large error bars on this value demonstrate the need for kinetic measurements. The observation¹⁵ of ketene product in low pressure, low temperature C₂H₂/O₂ flames offers some support for a rearrangement channel, but as it is not a direct kinetic measurement it is not conclusive. The rates of Ref. 15 are consistent with our extrapolation of the addition channel, but subsequent adduct reactions may be involved.

One final question is whether the possibility of a rearrangement channel at high temperature and low pressure is consistent with the lack of a significant room temperature, pressure-independent reaction. That is, can ketene production be the favored thermal decomposition pathway at 1000 K, while unstabilized C₂H₂OH* favors breakup to acetylene? (At low temperature and high pressure the collisionally stabilized adduct will be formed and persist.) For low pressure thermal decomposition k_0 prevails. The energy distribution of decomposing molecules peaks very close to the threshold. As Eq. (6) reveals, E_0 is the important variable, and the lowest energy pathway will be favored. Consider the second situation. The nonstabilized adducts C₂H₂OH* formed from OH addition to acetylene, however, are considerably excited. Their decomposition channel k_3 depends upon the relative $k(E)$ values for each pathway, which in turn depend upon the energy distribution and the two transition states. As k_3 is related to k_∞ , these relative rates depend upon both activation energies and A factors (ΔS^\ddagger). The rearrangement will have a tighter transition state than the decomposition reaction. Theoretical calculations²⁰ place the rearrangement transition state energy 5 kcal higher than that required for decomposition back to the OH and C₂H₂ reactants. Even if rearrangement were energetically favored, and thus would prevail for high temperature thermal decomposition, a favorably large A factor for decomposition may control the fate of unstabilized, hot adducts. Therefore it is possible for low pressure/high temperature decomposition to proceed through a rearrangement channel without requiring a large collisionless rearrangement channel at low temperatures.

There are however severe practical limits on the extent to which such an accommodation may be made. Equal barriers will produce $\sim 50\%$ decomposition of C₂H₂OH to ketone at low pressure 1000 K. The observed $< 10\%$ "direct" reaction channel at 300 K then requires a rearrangement transition state 4.6 e.u. tighter than that for decomposition to OH + C₂H₂. This is 2.2 e.u. tighter than the adduct and corresponds to C–OH frequencies of ~ 700 cm⁻¹. While we note that acetaldehyde has an entropy 5 e.u. greater than the isomeric ethylene oxide, the rearrangement transition state cannot be made much tighter than already required. These strictures, arising from theoretical considerations and the lack of a large room temperature, pressure independent rearrangement channel, indicate the adduct probably does not rearrange to a ketene precursor before decomposing at high temperatures. Decomposition back to reactants appears likely, but an experimental observation of equilibrium akin to that in the ethylene reaction¹³ would be useful.

This interpretation is well supported by the 1100 K LP/

LF data, which show no pressure dependence. The long dashed line in Fig. 4 is the extrapolated prediction for the addition channel, suggesting a significant rate pressure dependence over the range covered experimentally. However, when the thermal redissociation of the stable adduct is taken into account, the small, lower, short-dashed line is the predicted *net* formation rate for the adduct. The consistency of the experimental results with this latter prediction, plus the abstraction channel, indicates fast adduct decomposition without rearrangement above 1000 K, and suggests the addition channel is no longer of net significance.

G. Direct mechanisms

Data from this work and other investigations,^{5,6} coupled with the previous theoretical consideration of the addition channel, indicate an increasingly important direct reaction channel predominating above 1000 K. While production of ketene + H, CH₃ + CO, or H₂ + CHCO are all exothermic, they all require extensive atom rearrangement during a direct collision. Each requires at least four bond breaking or forming steps, and is likely to have a low *A* factor.

The endothermic hydrogen abstraction reaction to form H₂O and C₂H represents the most reasonable choice. The thermodynamic minimum for the activation energy is 6 kcal/mol. The exothermic OH + CH₄ reaction rate constant at high temperatures can be expressed as $2 \times 10^{-11} \exp(-2.5/RT)$ cm³ s⁻¹ indicating an added barrier of up to 2.5 kcal/mol is possible for abstraction. This places the acetylene abstraction activation energy in the 6–8 kcal/mol range. The *A* factor, which may be lower due to two fewer abstractable hydrogen atoms, should be near $1-2 \times 10^{-11}$ cm³ s⁻¹.

The line labeled *k_A* in Fig. 8, which follows the expression $2 \times 10^{-11} \exp(-9/RT)$, gives a reasonable agreement with existing data for the abstraction channel. These are our results near 1100 and 1300 K, and the conclusions of two flame studies near 1600⁶ and 2000 K.⁵ This is consistent with theoretical expectations, and indicates the importance of this reaction at acetylene flame temperatures. It also agrees with the small direct channel predicted by theory and suggested by the data at 900 K, as shown in Fig. 5. Coupled with the previous considerations of the declining addition channel, including the current measurements, this suggests abstraction is the dominant pathway above 1000–1400 K.

Our experiments alone cannot cover a large enough temperature range to determine accurate Arrhenius parameters for the direct channel. Recall in particular that the 1300 K results are less accurate than the measurements at 900 and 1100 K. A direct measurement at higher temperature is needed. By using our data points and the flame results^{5,6} at 1550 and 1850 K, Arrhenius parameters of $E_a = 14.3 \pm 1.9$ kcal/mol and $\log A = -9.9 \pm 0.3$ can be derived. This *A* factor, three to six times that for OH + CH₄, seems a bit too high. The *E_a* obtained, also higher than expected (14 vs 9), suggests either an additional barrier to alkyne hydrogen abstraction, a larger than expected acetylene bond energy, or an imprecisely determined temperature dependence. Our data by itself is consistent with either the theoretical or least squares Arrhenius parameters.

We note that five recent flame and modeling studies have included a direct OH + C₂H₂ reaction producing ketene in their mechanisms.²⁵ In addition, ketene has been observed¹⁵ in the post-flame region of acetylene systems. The 1500 K total OH + C₂H₂ rate constants used²⁵ varied from $1.4-6.5 \times 10^{-12}$ cm³ s⁻¹, while extrapolation of our measured value gives $\sim 1.1 \times 10^{-12}$ cm³ s⁻¹. It is of course difficult to prove a particular reaction channel from a complex kinetic system, especially when the data can be fit using differing rate constants and reaction products. It should be emphasized, however, that we have not detected the reaction products in this study. Such an effort is needed above 1200 K to properly understand the role of the OH + C₂H₂/reaction in flames.

IV. CONCLUSIONS

These LP/LF measurements of the OH + C₂H₂ reaction rate have furnished direct experimental evidence for an addition channel at 900 K and pressures of a few hundred Torr or more, but the dominance of a direct route at 1100 and 1300 K. The theoretical calculations for the addition channel rate constant illustrate the consistency of the lower temperature flow tube data and the LP/LF results and provide a coherent picture of the combined pressure and temperature dependence of this reaction rate from 200 to 1500 K. We note that Berman and Lin²⁶ have recently presented a similar analysis of the CH + N₂ reaction.

There remain several questions not directly addressed by this study. Although the calculations indicate ketene should be a relatively unimportant minor product, it has been detected (at unknown yield) in the mass spectroscopic study¹⁴ and in low-temperature flames.¹⁵ The indication of a direct rearrangement to ketene at low pressure in Ref. 3 is not directly refuted, although those overall data are described well by the simple addition channel without a ketene product. Here the 1 Torr point of Ref. 1 provides further evidence. The products of the direct reaction channel cannot be specified although the likely pathway would seem to yield H₂O + C₂H, the latter considered a soot precursor.

The form of the reaction rate as a function of temperature at a given pressure (Fig. 8) shows the need to consider the *combined* pressure and temperature dependence of addition reactions such as these when formulating a model of detailed combustion chemistry. The use of a simple Lindemann mechanism or a temperature-independent *k₀* is inadequate. For example, in the Nineteenth Combustion Symposium there were five papers²⁵ describing detailed kinetic models which included the OH + C₂H₂ reaction. A variety of reaction products and rate constant expressions and numerical values were used; none of the forms for *k₁* included the combined dependence on pressure and temperature although it is important in determining the value for conditions of interest in combustion.

Our calculations for the addition channel rate constant *k₁* and equilibrium constant *K₁* may be summarized by the following simple parametric fit, for direct use in modeling calculations:

$$\ln k_1 = A \ln P_{\text{eff}} - B, \quad (7)$$

where k_1 is in units of $10^{-12} \text{ cm}^{-3} \text{ s}^{-1}$ and P_{eff} is in Torr. Between 600 and 1000 K,

$$\begin{aligned} A &= 0.257 + 2.84 \times 10^{-4} T, \\ B &= -0.083 + 4.30 \times 10^{-3} T, \end{aligned} \quad (8)$$

and for T between 1000 and 1400 K,

$$\begin{aligned} A &= -0.231 + 7.73 \times 10^{-4} T, \\ B &= -3.37 + 7.58 \times 10^{-3} T. \end{aligned} \quad (9)$$

This reproduces our calculated values to within 10% for these temperatures:

$$\ln K_1 = 56.79 - 17130/T, \quad (10)$$

where K_1 in cm^{-3} describes the equilibrium constant between 600 and 1400 K. In Eq. (7), P_{eff} is given in terms of effective pressure referred to N₂, as we used in plotting the rate constants in Figs. 4 and 5. That is,

$$P_{\text{eff}} = \frac{P}{\beta_{\text{N}_2} Z_{\text{N}_2}} \sum_i \beta_i Z_i X_i, \quad (11)$$

where the β_i , Z_i , and X_i are the collision efficiency, collision frequency (e.g., Lennard-Jones) with adduct, and mole fraction of species i . Values of β_i can be obtained from studies of other unimolecular decomposition rates.¹⁰ There is considerable spread for a given collision partner in different reactions and this unfortunately represents a significant source of uncertainty in the use of Eqs. (7)–(11). Some representative values of $Z_i \beta_i / Z_{\text{N}_2} \beta_{\text{N}_2}$ for collision partners of likely importance in a combustion system, are taken from Ref. 10 and given as follows:



More work is still needed to understand this reaction fully. Our LP/LF measurements are probably accurate to 20%–30%. The calculations on the addition reaction represent a lengthy extrapolation and are expected to be good to within about a factor of 2 for any given temperature and pressure. Although the good agreement with the full set of low temperature results (Figs. 6 and 7) and the 900 K LP/LF results (Fig. 5) is gratifying, this fact must be borne in mind when accurate knowledge of k_1 is needed. More extensive, accurate data on the pressure and temperature dependence between 600 and 1000 K would be useful, and determinations below 10 Torr at lower temperatures would better fix k_0 . Product identification, particularly the yield of ketene at various temperatures, is needed, and the abstraction rate should be measured directly at higher temperatures. Finally, an equilibrium constant for the adduct should be determined. As a simple but significant system with many possible reaction paths, OH + C₂H₂ is also a good candidate for more detailed theoretical studies.

ACKNOWLEDGMENTS

We thank David Golden for useful discussions during the course of this work, including the suggestion that we undertake the calculation to supplement the experiments, and Roger Patrick for the use of his computer programs. This research was supported by the Department of Energy, Division of Basic Chemical Sciences on Contract No. DE-AC03-81ER10906.

- ¹A. Pastrana and R. W. Carr, Jr., *Int. J. Chem. Kinet.* **6**, 587 (1974).
- ²R. A. Perry, R. Atkinson, and J. N. Pitts, Jr. *J. Chem. Phys.* **67**, 5577 (1977).
- ³J. V. Michael, D. P. Nava, R. P. Borkowski, W. A. Payne, and J. L. Stief, *J. Chem. Phys.* **73**, 6108 (1980).
- ⁴R. A. Perry and D. Williamson, *Chem. Phys. Lett.* **93**, 331 (1982).
- ⁵C. P. Fenimore and G. W. Jones, *J. Chem. Phys.* **41**, 1887 (1964).
- ⁶W. G. Brown, R. P. Porter, J. D. Verlin, and A. W. Clark, *12th Symposium (International) on Combustion* (The Combustion Institute, Pittsburgh, 1969), p. 1035.
- ⁷P. W. Fairchild, G. P. Smith, and D. R. Crosley, *19th Symposium (International) on Combustion* (The Combustion Institute, Pittsburgh, 1982), p. 107.
- ⁸G. P. Smith, P. W. Fairchild, J. B. Jeffries, and D. R. Crosley, *J. Phys. Chem.* (to be published).
- ⁹J. Troe, *J. Chem. Phys.* **66**, 4758 (1977).
- ¹⁰J. Troe, *J. Phys. Chem.* **83**, 114 (1979).
- ¹¹P. W. Fairchild, G. P. Smith, and D. R. Crosley, *J. Chem. Phys.* **79**, 1795 (1983).
- ¹²L. Seaman, Final Report, SRI Project 6802, Menlo Park, California, August 1978.
- ¹³F. P. Tully, *Chem. Phys. Lett.* **96**, 148 (1983).
- ¹⁴J. R. Kanofsky, D. Lucas, F. Pruss, and D. Gutman, *J. Phys. Chem.* **78**, 311 (1974).
- ¹⁵J. Vandooren and J. P. van Tiggelen, *16th Symposium (International) on Combustion* (The Combustion Institute, Pittsburgh, 1977), p. 1133.
- ¹⁶T. Shimanouchi, *Tables of Molecular Vibrational Frequencies*, NSRDS-NDS No. 39, (U. S. GPO, Washington, D. C., 1972).
- ¹⁷*Handbook of Chemistry and Physics*, 61st ed. (Chemical Rubber, Boca Raton, 1980).
- ¹⁸S. W. Benson, *Thermochemical Kinetics*, 2nd ed. (Wiley, New York, 1976).
- ¹⁹D. F. McMillen and D. M. Golden, *Annu. Rev. Phys. Chem.* **33**, 493 (1982).
- ²⁰C. F. Melius and J. S. Binkley (private communication, 1984).
- ²¹*JANAF Thermochemical Tables*, NSRDS Natl. Bur. Stand. No. 37 (U. S. GPO, Washington, D. C., 1971).
- ²²J. O. Hirschfelder, C. F. Curtis, and R. B. Bird, *Molecular Theory of Gases and Liquids* (Wiley, New York, 1964).
- ²³M. J. Rossi, J. R. Pladziewicz, and J. R. Barker, *J. Chem. Phys.* **78**, 6695 (1983); H. Hippler, J. Troe, and H. J. Wendelken, *ibid.* **78**, 6709 (1983).
- ²⁴D. C. Tardy and B. S. Rabinovitch, *Chem. Rev.* **77**, 369 (1977); J. Troe, Ber. Bunsenges. Phys. Chem. **77**, 665 (1973); H. vandenBergh, N. Benoit-Guyot, and J. Troe, *Int. J. Chem. Kinet.* **9**, 223 (1977).
- ²⁵C. K. Westbrook, F. L. Dryer, and K. P. Schug, *Nineteenth Symposium (International) on Combustion* (The Combustion Institute, Pittsburgh, 1982), p. 153; J. M. Levy, R. Taylor, J. P. Longwell, and A. F. Sarofim, *ibid.*, p. 167; J. A. Miller, R. E. Mitchell, M. D. Smooke and R. J. Kee, *ibid.*, p. 181; J. Warnatz, H. Bockborn, A. Möser and H. W. Wenz, *ibid.*, p. 197; J. D. Bittner and J. B. Howard, *ibid.*, p. 211.
- ²⁶M. R. Berman and M. C. Lin, *J. Phys. Chem.* **87**, 3933 (1983).